Advances in Energy Research, *Vol. 5, No. 3 (2017) 255-275*
DOI: https://doi.org/10.12989/eri.2017.5.3.255

Sensitivity analysis of numerical schemes in natural cooling flows for low power research reactors

Imaneh Karami and Mahdi Aghaie*

Department of Engineering, Shahid Beheshti University, G.C, P.O.Box 1983963113, Tehran, Iran

(Received April 26, 2018, Revised June 21, 2018, Accepted June 22, 2018)

Abstract. The advantages of using natural circulation (NC) as a cooling system, has prompted the worldwide development to investigate this phenomenon more than before. The interesting application of the NC in low power experimental facilities and research reactors, highlights the obligation of study in these laminar flows. The inherent oscillations of NC between hot source and cold sink in low Grashof numbers necessitates stability analysis of cooling flow with experimental or numerical schemes. For this type of analysis, numerical methods could be implemented to desired mass, momentum and energy equations as an efficient instrument for predicting the behavior of the flow field. In this work, using the explicit, implicit and Crank-Nicolson methods, the fluid flow parameters in a natural circulation experimental test loop are obtained and the sensitivity of solving approaches are discussed. In this way, at first, the steady state and transient results from explicit are obtained and compared with experimental data. The implicit and crank-Nicolson scheme is investigated in next steps and in subsequent this research is focused on the numerical aspects of instability prediction for these schemes. In the following, the assessment of the flow behavior with coarse and fine mesh sizes and time-steps has been reported and the numerical schemes convergence are compared. For more detail research, the natural circulation of fluid was modeled by ANSYS-CFX software and results for the experimental loop are shown. Finally, the stability map for rectangular closed loop was obtained with employing the Nyquist criterion.

Keywords: natural circulation; single-phase; numerical methods; low Grashof; CFD; experimental facility

1. Introduction

Natural circulation loop refers to the geometrically separated heat sink and source but thermally connected via the fluid flow. The fluid flow is the results of the buoyancy force due to the density difference across the heat sink named heater and the heat source named cooler and the difference in elevation between these two locations. Such this loop also is named natural circulation or thermosyphon.

It can be considered suitable for many engineering applications such as: Nuclear reactors, geothermal systems, electronic systems cooling, solar heaters and cooling systems (Ibrahim *et al.* 2015, Tyurina and Mednikov 2015). In nuclear reactors when heat removal system does not operate properly due to the power failure or the technical malfunction of the pumps, natural

*Corresponding author, Ph.D., E-mail: m_aghaie@sbu.ac.ir

http://www.techno-press.org/?journal=eri&subpage=7 ISSN: 2287-6316 (Print), 2287-6324 (Online)

circulation prevents damage of excess heat into the core (Zvirin 1982, Dauria and Frogheri 2002, Deokattey *et al.* 2013, Bahonar and Aghaie 2017). Therefore, making an allowance for flow parameters such as flow rate and heat distribution, which are the main parameters in the natural circulation loop, are very important. Single-phase natural circulation has been studied in many papers in various topics (Guk and Kalkan 2015, Zvirin *et al.* 1981, Nayak *et al.* 1995, Vijayan 2002, Vijayan and Nayak 2005, Misale *et al.* 2007, Ruppersberg *et al.* 2007, Ambrosini 2003, Vijayan 2007, Muscato and Xibilia 2003, Jafari *et al.* 2003). The rectangular loop is used in most of the articles such as Vijayan (2002), Mousavian *et al.* (2004) and Fichera *et al.*, (2003). Welander (1967) and also Zvirin and Grief (1979) have considered a method to use for studying natural circulation in a loop with two vertical branches and a point source and sink. Equations of mass, energy and momentum for the natural circulation loop have been investigated extensively using explicit finite difference method; it has been studied by Welander (1967), Huang and Zelaya (1988), Ambrosini (2000), Vijayan (2002) and Mousavian *et al.* (2004). Considering uniform heat flux at the heat source and isothermal heat sink can be found in Vijayan *et al.* (1992), Mousavian (2004) and Ambrosini (2000). The Japikse (1973) and Metrol and Greif (1985) have investigated single-phase natural circulation generally. The TMI accident in the nuclear industry in 1979 showed that the best effective way to remove heat from core is natural circulation of fluid. For this, Zvirin and Grief in 1979 studied, transient behavior of natural circulation in a test loop with thermal point heat sink and heat source. After that, Tolman *et al.* (1988) presented new studies about this accident. Generally, analyzing of the transient behavior of the fluid dynamic systems with finite difference methods is very sensitive on the effects of discretization of partial differential equations (PDE). In some cases, these effects may gradually change quality of theory camper with exact solution, or experiments. In this paper, transient analysis of natural circulation has been studied numerically. The governing equations are discrete by the finite difference methods, explicit, full implicit and Cranck-Nicolson. The numerical results for some cases are obtained and the sensitivity of them are shown. Afterwards, the natural circulation loop is simulated by ANSYS CFX and the results are reviewed by experimental data for a rectangular loop. The CFD software provided very favorable results in the analysis of natural circulation (Pilkhwal *et al.* 2007, Kumar *et al.* 2011, Safavi *et al.* 2012, Wang *et al.* 2013). ANSYS CFX (Ansys Inc. 2010) is well-known for its advanced solver technology cause to achieving reliable and accurate solutions quickly and robustly.

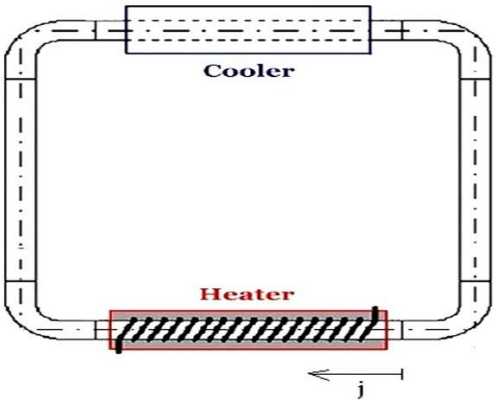

Fig. 1 Schematic diagram of rectangular closed loop

Table 1 Geometric dimensions

Parameter	Value (cm)
Height of loop	124.5
Width of loop	148
Inner diameter of loop	4
Length of heating section	140
Length of cooling section	120
Inner diameter of cooler	20

2. Mathematical model

The desired assumptions in the governing equations are; a) In all this process diameter of the loop is constant, b) fluid is considered single-phase and incompressible, c) The equations are solved in one dimension. In the wok, a simple uniform diameter rectangular loop is considered with both horizontal heater and cooler connected by adiabatic pipes as shown in Fig. 1. Table 1 shows main dimensions of the loop.

Assuming the coordinate j runs around the loop with the origin at the heater inlet, one-dimensional single-phase mass, momentum and energy equations can be written as

$$\frac{\partial W}{\partial j} = 0 \tag{1}$$

$$\frac{L_t}{A}\frac{dW}{dt} = g\oint \rho dz - \frac{fL_t W^2}{2D\rho A^2} \tag{2}$$

$$\frac{\partial T}{\partial t} + \frac{W}{A\rho_0}\frac{\partial T}{\partial j} = \begin{cases} \dfrac{4q}{D\rho_0 C_p} & \text{for heater} \\ 0 & \text{for legs} \\ -\dfrac{4U}{D\rho_0 C_p}(T - T_s) & \text{for cooler} \end{cases} \tag{3}$$

The heat flux (q) is assumed as a constant at the heater source and the rate of cooling water in the secondary side of the cooler is taken as a constant temperature (T_s). For studding, the behavior of the system non-dimensional group can be used that be seen below

$$w = \frac{W}{W_{ss}};\ \theta = \frac{T - T_s}{(\Delta T_h)_{ss}};\ \tau = \frac{t}{t_r};\ J = \frac{j}{H};\ Z = \frac{z}{H} \tag{4}$$

Therefore, the equation in non-dimensional form would be of the form

$$\frac{dw}{d\tau} = \frac{Gr}{\mathrm{Re}_{ss}^2}\oint \theta dZ - \frac{PL_t w^{2-b}}{2D\,\mathrm{Re}_{ss}^b} \tag{5}$$

$$\frac{\partial \theta}{\partial \tau} + \left(\frac{L_t}{H}\right)w\frac{\partial \theta}{\partial J} = \begin{cases} \dfrac{L_t}{L_h} & \text{for heater} \\ 0 & \text{for legs} \\ -St_m\theta & \text{for cooler} \end{cases} \tag{6}$$

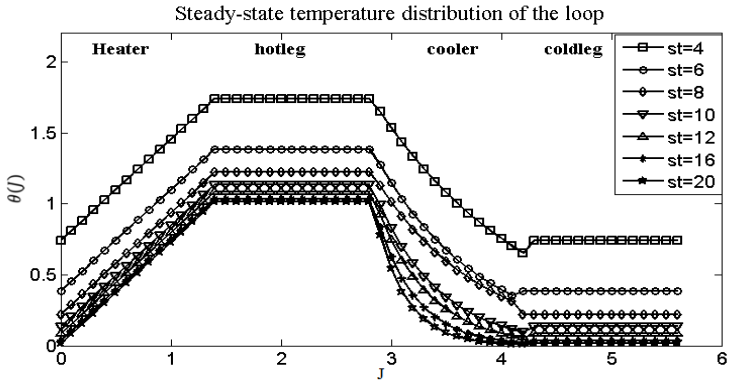

Fig. 2 Steady-state temperature distribution along the loop

where non-dimensional parameters are

$$\mathrm{Re}=\frac{WD}{\mu A};\ pr=\frac{\mu C_p}{k};\ Nu=\frac{UL_t}{k};\ St=\frac{UA}{C_pW};\ St_m=\frac{4Nu}{\mathrm{Re}_{ss}.pr};\ Gr=\frac{g\beta D^3\rho_0^2Q_hH}{A\mu^3C_p} \tag{7}$$

Friction factor is obtained according to the Darcy-Weisbach relation which is similar to Eq. (8), it can be used in the momentum equation

$$f=\frac{P}{\mathrm{Re}^b} \tag{8}$$

where P=64 and b=1 for laminar flow and P=0.316 and b=0.25 for turbulent flow using the Blassius correlation.

2.1 Steady state

By solving the energy and momentum equations in steady state condition, the temperature distribution and steady Reynolds number within the loop would be

$$\theta_{heater}=\theta_{cl}+\frac{H}{L_t}J \tag{9}$$

$$\theta_{cooler}=\theta_{hl}e^{\frac{St_mH}{L_t}(J_{hl}-J)} \tag{10}$$

$$\mathrm{Re}_{ss}=[\frac{2}{P}Gr\frac{D}{L_t}\oint[\theta(J)]_{ss}]^{\frac{1}{3-b}} \tag{11}$$

If the outlet temperature of heater and cooler are chosen to be the same as with cold and hot legs temperatures in the loop, respectively, legs temperatures at the steady state condition can then be obtained by solving the Eq. (10) at $S=S_c$ and $S=S_h$

$$\theta_{cooler}=\theta_{hl}e^{\frac{St_mH}{L_t}L_c}=\theta_{cl} \tag{12}$$

$$\theta = \theta_{cl} + 1 = \theta_{hl} \tag{13}$$

So the temperature of legs would be

$$\theta_{cl} = \frac{1}{e^{\frac{St_m}{L_t}L_c} - 1} \quad \text{and} \quad \theta_{hl} = \frac{1}{1 - e^{-\frac{St_m}{L_t}L_c}} \tag{14}$$

The temperature distribution of the different parts of the loop is shown in Fig. 2. These were obtained for different values of Stanton number.

2.2 Transient analysis

The Eqs. (5) and (6) are numerically solved with finite difference method (FDM). A backward difference approximation that is first order accurate is used to discrete equations in space and three types of temporal discretization; explicit, implicit and Crank-Nicolson methods are applied for integration in time. In the following the implementation of three types of time integrations and comparison with the experimental data are shown.

2.2.1 Explicit method

If is assumed that the time level n is known and time level n+1 is unknown then the finite difference formulation of the Eq. (5) and (6) in explicit form are

$$\begin{cases} \text{Heater: } \theta_{i,n+1} = (1 - \frac{L_t \Delta\tau}{H \Delta J} w_n)\theta_{i,n} + (\frac{L_t \Delta\tau}{H \Delta J} w_n)\theta_{i-1,n} + \frac{L_t \Delta\tau}{L_h} \\ \text{Cooler: } \theta_{i,n+1} = (1 - \frac{L_t \Delta\tau}{H \Delta J} w_n - St_m \Delta\tau)\theta_{i,n} + (\frac{L_t \Delta\tau}{H \Delta J} w_n)\theta_{i-1,n} \\ \text{Vertical legs: } \theta_{i,n+1} = (1 - \frac{L_t \Delta\tau}{H \Delta J} w_n)\theta_{i,n} + (\frac{L_t \Delta\tau}{H \Delta J} w_n)\theta_{i-1,n} \end{cases} \tag{15}$$

$$w^{n+1} + \frac{PL_t \Delta\tau}{2D \operatorname{Re}_{ss}^b}(w^{n+1})^{2-b} = w^n + \frac{Gr \Delta\tau}{\operatorname{Re}_{ss}^3} \oint \theta_{i,n+1} dz \tag{16}$$

Note that the following convergence condition should be fulfilled.

$$\Delta\tau \le \frac{1}{(\frac{L_t w_n}{H \Delta J}) + St_m} \tag{17}$$

Generally, the flow in a natural circulation loop has inherent oscillations. The difference in density due to temperature changes causes fluid flow. The fluid heated in heater and the force caused by the difference in density and height, raises the fluid along the hot leg. If the transferred power to raise fluid, overcomes the friction force and gravity, the fluid goes up along the loop, after arriving to the cooler, fluid temperature dropped and goes down along the cold leg, then again heated in heater and this process will continue. On the contrary, if the power of the heater is not enough, the flow is unstable and studying of this issue has been investigated in this paper. The behavior of the flow can be in different forms like what is shown in Fig. 3.

The behavior of dimensionless mass flow (w) for a rectangular loop in different Grashof numbers is in three modes. They are stable, neutral and unstable (Gr=5E10, 3.5E10, 2.5E10

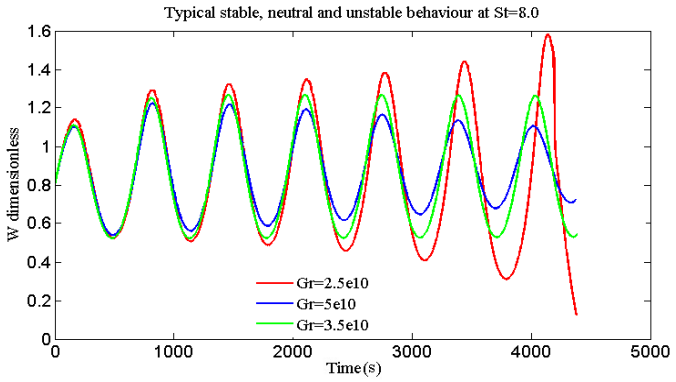

Fig. 3 Typical stable, neutral and unstable behavior at St=8.0

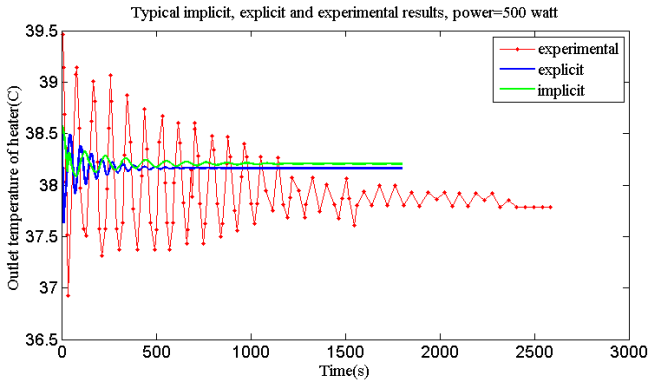

Fig. 4 Typical explicit, implicit and at heat power=500 watt, and experimental data

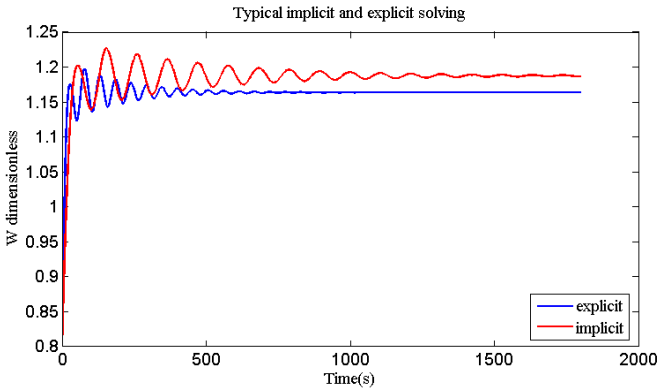

Fig. 5 Explicit and implicit dimensionless mass flow

respectively). The flow obtains its power from the heater because it is the source of the driving head is created due to the density difference. If the power and therefore the force for fluid flow are not enough, flow reversal occurs. It is when the oscillations are amplified by the time in the diagram, what can be seen in Fig. 3, so it becomes unstable. The behavior of the flow at about 100 Watts and higher (i.e., the power of electrical heater, Gr=5E10) becomes stable.

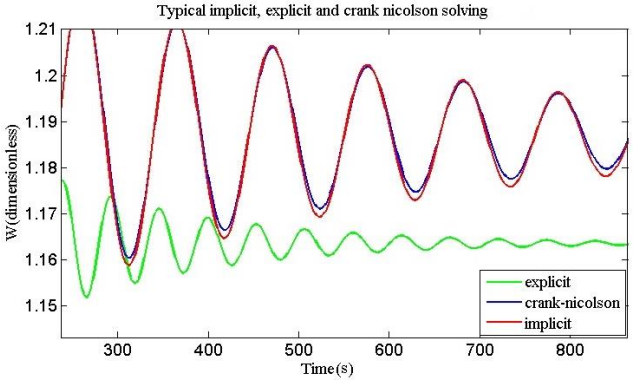

Fig. 6 Typical explicit, implicit and Crank-Nicolson at heat power=100 watt

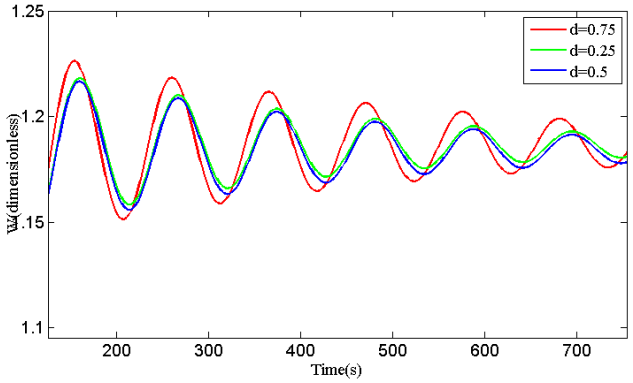

Fig. 7 Crank-Nicolson results at d=0.25, 0.5, 0.75

2.2.2 Implicit formulation

When the spatially discretized equations are considered at time level n+1, the final form of the discretized equations would be of the form

$$\begin{cases} \text{Heater: } (1+\frac{L_t\Delta\tau}{H\Delta J}w_n)\theta_{i,n+1}-(\frac{L_t\Delta\tau}{H\Delta J}w_n)\theta_{i-1,n+1}=\theta_{i,n}+\frac{L_t\Delta\tau}{L_h} \\ \text{Cooler: } (1+\frac{L_t\Delta\tau}{H\Delta J}w_n+St_m\Delta\tau)\theta_{i,n+1}-(\frac{L_t\Delta\tau}{H\Delta J}w_n)\theta_{i-1,n+1}=\theta_{i,n} \\ \text{Vertical legs: } (1+\frac{L_t\Delta\tau}{H\Delta J}w_n)\theta_{i,n+1}-(\frac{L_t\Delta\tau}{H\Delta J}w_n)\theta_{i-1,n+1}=\theta_{i,n} \end{cases} \tag{18}$$

$$w^{n+1}+\frac{PL_t\Delta\tau}{2D\,\mathrm{Re}_{ss}^{b}}(w^{n+1})^{2-b}=w^{n}+\frac{Gr\Delta\tau}{\mathrm{Re}_{ss}^{3}}\oint\theta_{i,n+1}dz \tag{19}$$

The comparison of outlet temperature distribution of the heater for explicit, implicit solution and experimental data is depicted in Fig. 4. Dimensionless flow rates are shown in Fig. 5 for 500-watt heat power.

2.2.3. Crank Nicolson

This method is an unconditionally stable implicit method with second order accuracy in time.

By applying a combination of the forward Euler method at time level n and backward Euler method at time level n+1, the finite difference formulation of the equations are given as

Heater:

$$(1+d\frac{L_t\Delta\tau}{H\Delta J}w_n)\theta_{i,n+1}-(d\frac{L_t\Delta\tau}{H\Delta J}w_n)\theta_{i-1,n+1}+((1-d)\frac{L_t\Delta\tau}{H\Delta J}w_n-1)\theta_{i,n}-((1-d)\frac{L_t\Delta\tau}{H\Delta J}w_n)\theta_{i-1,n}=\frac{L_t\Delta\tau}{L_h} \tag{20}$$

Cooler:

$$(1+d\frac{L_t\Delta\tau}{H\Delta J}w_n+d St_m\Delta\tau)\theta_{i,n+1}-(d\frac{L_t\Delta\tau}{H\Delta J}w_n)\theta_{i-1,n+1}+((1-d)\frac{L_t\Delta\tau}{H\Delta J}w_n+(1-d)St_m\Delta\tau-1)\theta_{i,n}$$
$$-(d\frac{L_t\Delta\tau}{H\Delta J}w_n)\theta_{i-1,n}=0 \tag{21}$$

Vertical legs:

$$(1+d\frac{L_t\Delta\tau}{H\Delta J}w_n)\theta_{i,n+1}-(d\frac{L_t\Delta\tau}{H\Delta J}w_n)\theta_{i-1,n+1}+(1-(1-d)\frac{L_t\Delta\tau}{H\Delta J}w_n)\theta_{i,n}+((1-d)\frac{L_t\Delta\tau}{H\Delta J}w_n)\theta_{i-1,n}=0 \tag{22}$$

$$w^{n+1}+\frac{PL_t\Delta\tau}{2D\,\mathrm{Re}_{ss}^{b}}(w^{n+1})^{2-b}=w^{n}+\frac{Gr\Delta\tau}{\mathrm{Re}_{ss}^{3}}\oint\theta_{i,n+1}dz \tag{23}$$

The equations of temperature distribution and momentum have been discretized by three different methods of (FDM). These three methods have been compared and shown in Fig. 6 for 100-watt heat power. Also comparing of different d (dividing coefficient in Crank Nicolson) is seen in Fig. 7.

This part of the research is focused on the numerical aspects of stability and instability prediction. Mesh size, Δj, has been considered for studying what plays an important role in the behavior of different parameters in the natural circulation loop. Coarse nodalization has been adopted with 100 mm mesh size. 10 mm has been used for fine nodalization too. The typical behavior of dimensionless mass flow (w) for rectangular loop in different Grashof numbers was shown in Fig. 3. Depending on the heater power without change in amount of the friction and elevation between heater and cooler, flow in the loop may show stable or unstable behavior. The flow was unstable for Gr=2.5e10 or in about 85-watt power of the heater. The calculation has been started by initializing the fluid temperature distributions at steady state conditions with the 85-watt

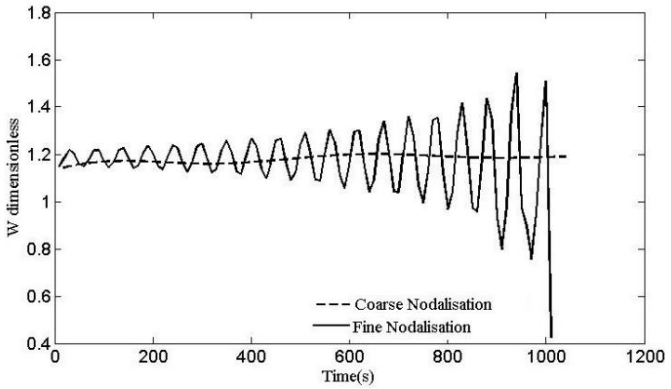

Fig. 8 Dimensionless massflow for the explicit type with two different nodalisation

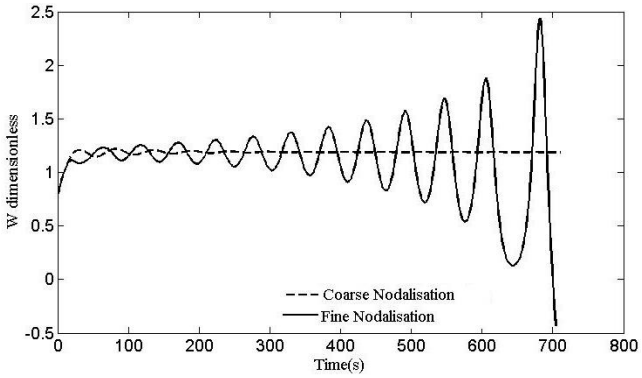

Fig. 9 Dimensionless mass flow for the implicit type with two different nodalization

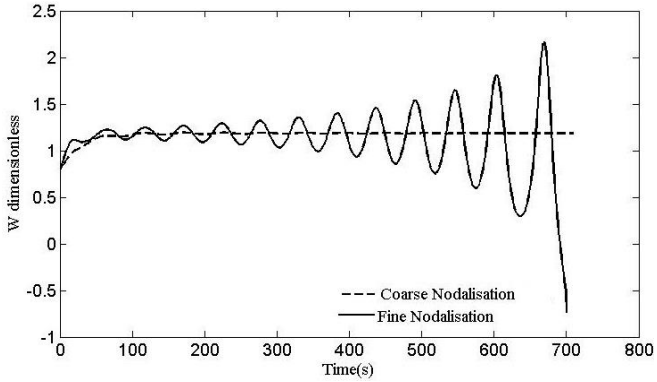

Fig. 10 Dimensionless mass flow for the crank-Nicolson type with two different nodalization

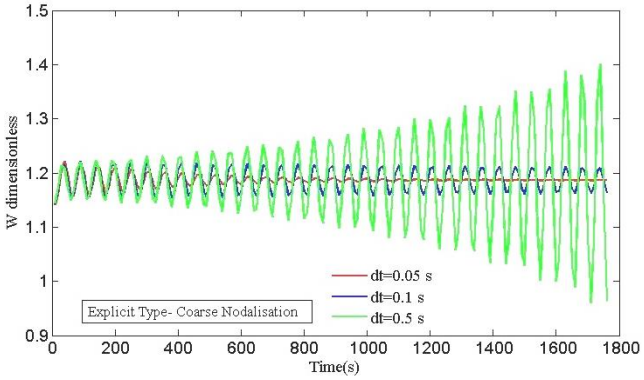

Fig. 11 Dimensionless mass flow for the explicit type with three different time steps

heater power. It could be found that the coarse nodalization was unable to predict the actually instability and the fine nodalization allowed predicting a physical unstable behavior. Fine and coarse nodalization have been considered in the present work too. The behavior of the system as predicted by three different numerical methods described in pervious section has been investigatedtoo. The results of explicit solution for two different nodalization with the time step

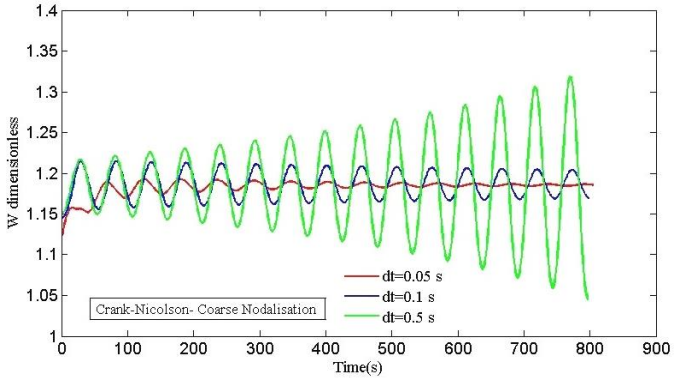

Fig. 12 Dimensionless mass flow for the implicit type with three different time steps

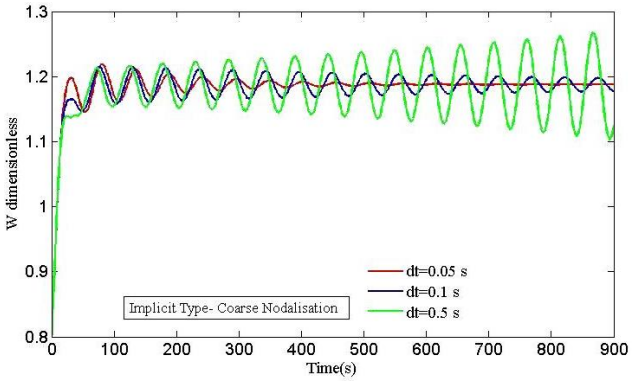

Fig. 13 Dimensionless mass flow for the crank-Nicolson type with three different time steps

Δt=0.1 s are shown in Fig. 8.

Instability can be seen in with fine nodalization. In particular, the use of coarse nodalization results in the prediction of a stable behavior, while the fine nodalization leads to correct instability. The prediction with Implicit and Crank-Nicolson, reported in Fig. 9 and Fig. 10 is the same.

Figs. 11, 12 and 13 show the results obtained by Explicit, Implicit and Crank-Nicolson with the coarse nodalization for three time steps: 0.05 s, 0.1 s and 0.5 s (Gr=2.5e10 or in about 85 watt). It is for investigating the effect of the time-step on the prediction of stability behavior. In Explicit type (Fig. 11), the effect of increasing the time step from 0.1 s to 0.5 s is considerable but oscillations are very weak by decreasing Δt from 0.1 s to 0.05 s. It is for changing in numerical dissipation. The other types, Implicit and Crank-Nicolson are less sensitive to the changes in time-step (Figs. 12 and 13).

3. The algorithm of numerical solution

The numerical solution of energy and momentum equations with finite difference method as was explain before will be shown in Fig. 14.

The equations will be solved and the results have been investigated for initial condition of

transient solution. The temperature can be obtained from energy equation and used for momentum equation. So dimensionless flow rate is obtained in the same time. Then the next time step will be investigated and the process can be repeated. In any time steps, the initial dimensionless temperature and flow rate are the values were obtained from previous time step. In explicit method, applying the numerical stability criterion expressed in Eq. (17), is important.

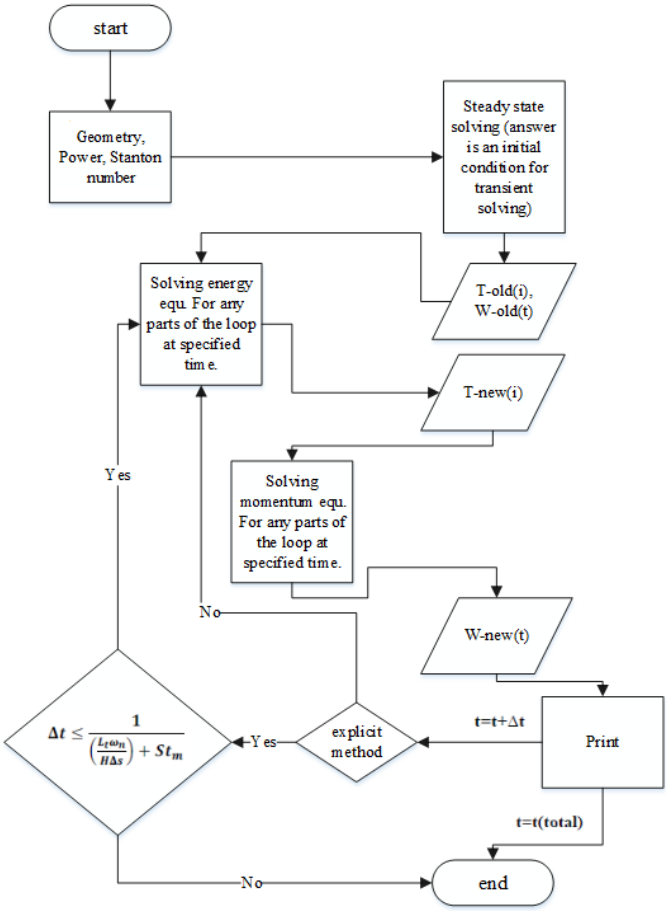

Fig. 14 The algorithm of numerical solution

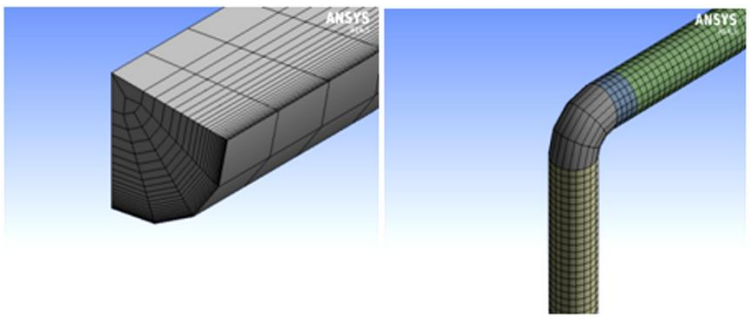

Fig. 15 Typical mesh model of the loop

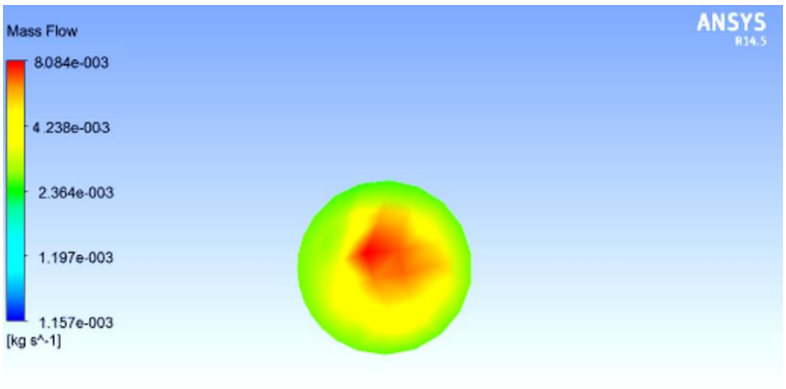

Fig. 16 Mass flow rate at time=2500 (s)

Table 2 Results for flow rate

Time(s)	Integral on the cross-section(kg/s) CFX	Numerical data(kg/s)	Relative error %
2500	4.8e-3	5.1e-3	0.05

4. The ANSYS CFX simulation

In this work, ANSYS.V14.5 software is used for modeling and analysis of rectangular natural circulation loop. The loop is designed as a simple model and meshed for analyzing. Meshing is one of the critical stages of the simulation and should be carried out according to the geometry of each location. The meshing of the rectangular loop is developed in Fig. 15.

The initial conditions for solving the problem are very important, if approximation for the initial conditions were away from reality, the resulting values would be wrong. For a transient solution, the best values for initial condition are the values obtained from the steady-state solution. This software makes it possible for the user to define two configurations that the first is initial condition for the second. Depending on the problem and its solution users can be define any of configuration to solve. After 2500 seconds flow rate obtaining of CFX is shown in Fig. 16.
The result of integrating on the cross section of leg is compared with numerical solutions for the power of 100 watt in Table 2.

After solving the equations, the temperature distribution and fluid flow can be observed across the loop at any time. It can be obviously seen in Fig. 17. The program runs for 3000 seconds and reslts are shown in 6 different steps to compare the flow in different times. The flow direction is determined by changing the temperature, with changing the temperature over the loop and at any time, the density changes and the fluid is flowed.

For example, in the first step, after 120 seconds that the transient state started, the fluid flow is an counterclockwise, because the temperature is increasing to the right of the heater, it is observed that the temperature is decreasing by moving along the cooler from right to left. from left to right across the heater, the density decreases with increasing temperature, the fluid becomes light and therefore the force for moving along the right leg obtained from density variation, then fluid moves up to reach the cooler, the temperature decreases in the cooler, increases its density so move down the left leg. In other steps, the fluid flow can be explained in the same way. The flow instability is observed in the first seconds. At first, the flow is counterclockwise and after several

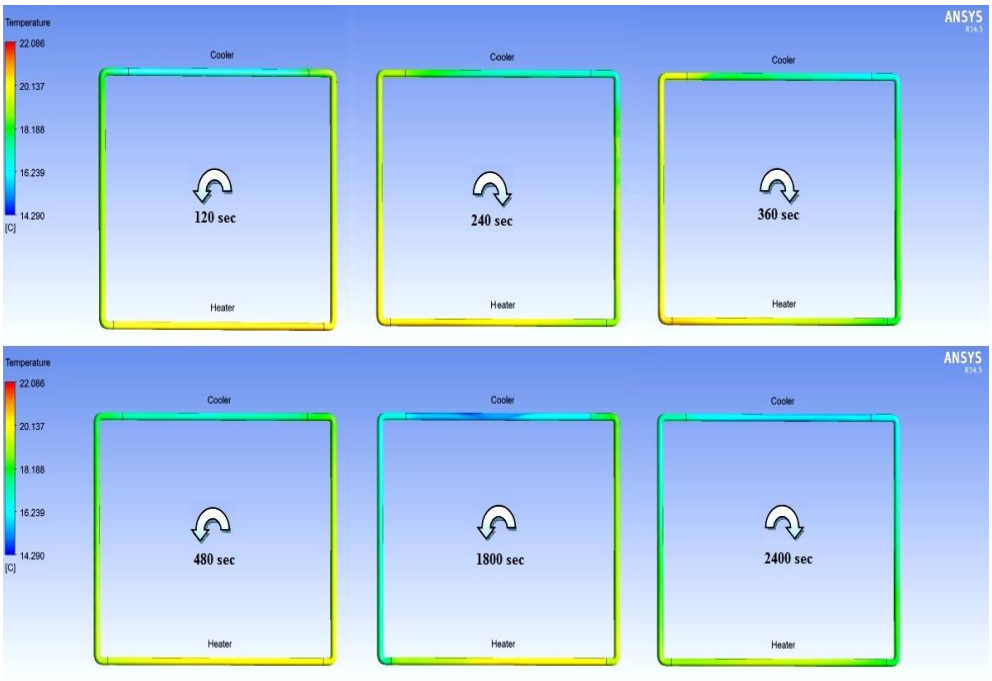

Fig. 17 Temperature distributions and fluid flow, power:100-watt

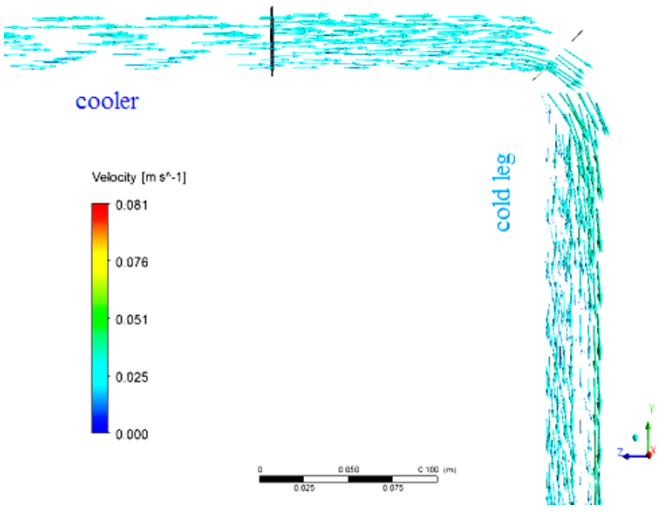

Fig. 18 Flow vectors on the axial plan of heater

steps it becomes clockwise and stable (after 2400 second).

Velocity of the fluid in cold leg where it is going down is shown in Fig. 18. Average velocity of the fluid flow is 0.06 m/s approximately for 500-watt heat power.

The temperature distribution of this power is shown in Fig. 19 for this power. For 500-watt power of heater available experimental data was compared with results of ANSYS-CFX in Fig. 20.

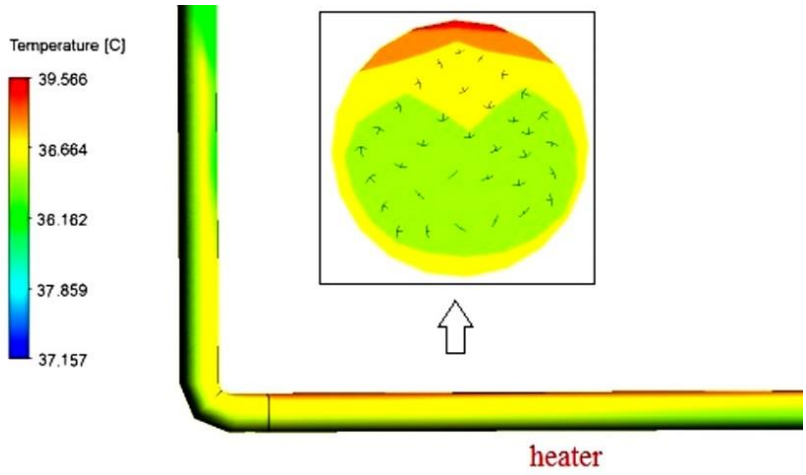

Fig. 19 Temperature distributions of heater and cross-section of it at heat power=500 watt

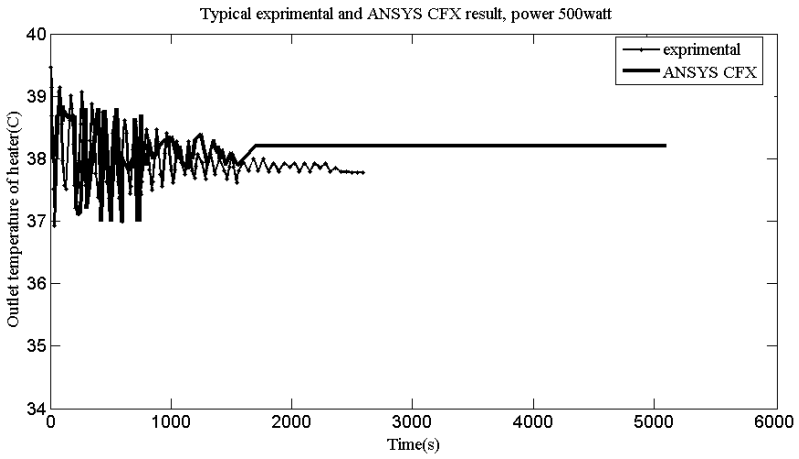

Fig. 20 Typical result of ANSYS-CFX and experimental data

5. Stability analysis

The natural circulation systems used in the industry should operate in a stable position. Therefore, the operation of the natural circulation system must be limited to this state. So, it is necessary to examine two stable and unstable areas for the natural circulation system.

For studying the stability, stability maps are obtained as a function of non-dimensional modified Grashof and Stanton numbers. The linear method and the Nyquist stability criterion is used in this analysis.

In linear analysis, the flow stability tests by creating a perturbation in temperature and mass flow rate. So the transient dimensionless mass flow rate and temperatures in the momentum and energy equations should be perturbed as

$$\theta = \theta_{ss} + \theta' \quad \text{and} \quad w = w_{ss} + w' \tag{24}$$

Applying these into the Eqs. (5) and (6) the perturbed momentum and energy equations would be

$$\frac{dw'}{d\tau}=\frac{Gr_m}{Re_{ss}^3}\oint\theta'\,dZ-\frac{pL_t(2-b)w'}{2DRe_{ss}^b} \tag{25}$$

$$\begin{cases}\dfrac{\partial\theta'}{\partial\tau}+\varphi\dfrac{\partial\theta'}{\partial\tau}+\dfrac{L_t}{L_h}w'=0 & \text{for heater}\\ \dfrac{\partial\theta'}{\partial\tau}+\varphi\dfrac{\partial\theta'}{\partial\tau}=0 & \text{for legs}\\ \dfrac{\partial\theta'}{\partial\tau}+\varphi\dfrac{\partial\theta'}{\partial\tau}+St_m(\theta'-w'\theta_{ss})=0 & \text{for cooler}\end{cases} \tag{26}$$

If small perturbations are defined as an exponential function

$$w'=\bar{w}\varepsilon e^{n\tau}\quad\text{and}\quad\theta'=\bar{\theta}(J)\varepsilon e^{n\tau} \tag{27}$$

Applying these expressions into the Eqs. (25) and (26), the equations would be

$$n-\frac{Gr_m}{Re_{ss}^3}\frac{\bar{I}}{\bar{w}}+\frac{pL_t(2-b)}{2DRe_{ss}^b}=0 \tag{28}$$

$$\begin{cases}\dfrac{d\bar{\theta}(J)}{dS}+\dfrac{n}{\varphi}\bar{\theta}(J)+\dfrac{L_t\bar{w}}{\varphi L_h}=0 & \text{for heater}\\ \dfrac{d\bar{\theta}(J)}{dS}+\dfrac{n}{\varphi}\bar{\theta}(J)=0 & \text{for legs}\\ \dfrac{d\bar{\theta}(J)}{dS}+\left(\dfrac{n+St_m}{\varphi}\right)\bar{\theta}(J)-\dfrac{St_m\theta_{ss}\bar{w}}{\varphi}=0 & \text{for cooler}\end{cases} \tag{29}$$

$$\bar{I}=\int\bar{\theta}(J)dZ \tag{30}$$

At first, by solving the ordinary differential Eqs. (29). $\bar{\theta}(J)$ in $J=J_h$, $J=J_{hl}$, $J=J_c$ and $J=J_t$ obtained.

$$\frac{\bar{\theta}_{cl}}{\bar{w}}=\frac{St_m(\theta_{hl})_{ss}\,e^{\frac{n(L_t+L_{cl})}{L_t}}\left(1-e^{\frac{-nL_c}{L_t}}\right)+\frac{L_t}{L_h}\left(1-e^{\frac{nL_h}{L_t}}\right)}{n(e^{\frac{st_mL_c+nL_t}{L_t}}-1)} \tag{31}$$

$$\frac{\bar{\theta}_h}{\bar{w}}=\frac{St_m(\theta_{hl})_{ss}\,e^{\frac{nL_{hl}}{L_t}}\left(e^{\frac{nL_c}{L_t}}-1\right)+\frac{L_t}{L_h}\left(e^{\frac{-nL_h}{L_t}}-1\right)e^{\frac{(st_mL_c+nL_t)}{L_t}}}{n\left(e^{\frac{st_mL_c+nL_t}{L_t}}-1\right)} \tag{32}$$

$$\frac{\bar{\theta}_{hl}}{\bar{w}}=\frac{St_m(\theta_{hl})_{ss}\left(e^{n\frac{L_c}{L_t}}-1\right)+\frac{L_t}{L_h}e^{\frac{st_mL_c+n(L_t-L_{hl})}{L_t}}\left(e^{-n\frac{L_h}{L_t}}-1\right)}{n\left(e^{\frac{st_mL_c+nL_t}{L_t}}-1\right)} \tag{33}$$

$$\frac{\bar{\theta}_c}{\bar{w}} = \frac{St_m\left(\theta_{hl}\right)_{ss} e^n\left(1-e^{\frac{-nL_c}{L_t}}\right)+\frac{L_t}{L_h}e^{\frac{nL_{cl}}{L_t}}\left(1-e^{\frac{nL_h}{L_t}}\right)}{n\left(e^{\frac{st_m L_c+nL_t}{L_t}}-1\right)} \tag{34}$$

So $\bar{I}$ can be observed from Equ. (30). The stability map for rectangular closed loop will be dependent on the characteristics equation can be expressed as

$$F(n)=n-\frac{Gr_m}{Re_{ss}^3}\frac{\bar{I}}{\bar{w}}+\frac{pL_t(2-b)}{2DRe_{ss}^b}=0 \tag{35}$$

Employing the Nyquist stability criterion for solving Eq. (35) will obtain stability map. The positive roots of the characteristics equation can obtain unstable conditions. So the margin of stable and unstable regions can be observed in stability map for rectangular closed loop. Typical plots based on the Nyquist criterion is shown in Fig. 20. In Figs. 20(a)-20(c) the Grashof number is constant and Stanton numbers change. However, in Figs. 20(d)-20(f) while Grashof numbers change, the Stanton number is constant. The roots of the characteristics equation that obtain stability map are shown in Fig. 21.

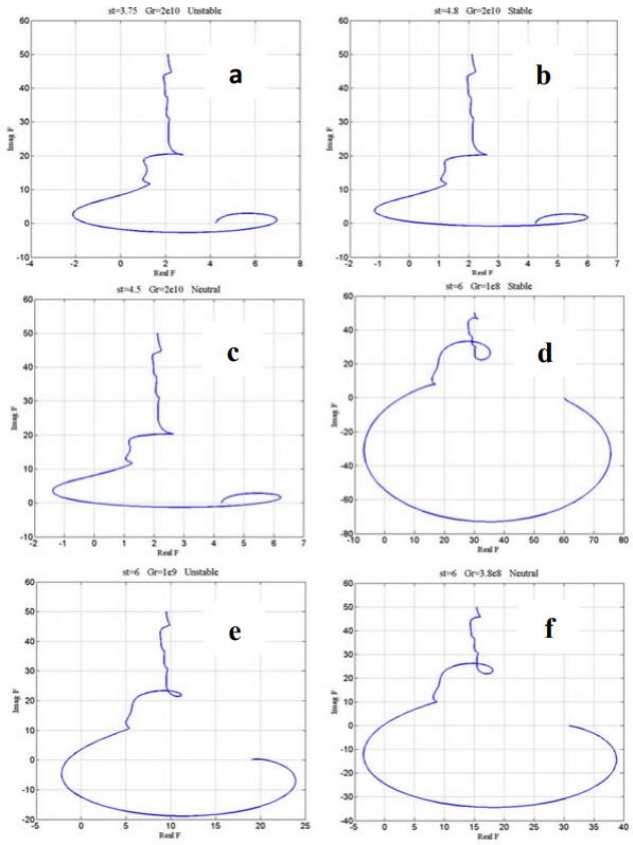

Fig. 21 Behavior of stability, neutral and un-stability using Nyquist criterion

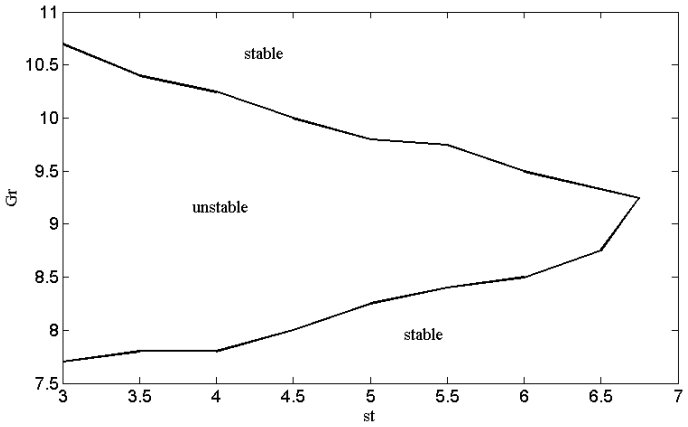

Fig. 21 Stability map of rectangular closed loop

6. Conclusions

This work focused on utilizing different finite-difference methods to solving mass, momentum and energy equations for the rectangular natural circulation closed loop. At last the loop was modeled with linear analysis using perturbation method. At first explicit type of equations were considered and solved in the steady-state and transient, the results showed good agreement with experimental data. Then results were obtained by solving equations in implicit and Crank-Nicolson format. Comparing explicit and implicit methods shows oscillations in explicit type are less than implicit and this method is quicker to respond but a convergence condition is needed. Flow oscillations are not resulting of the numerical solution only; a fluid flow has inherent oscillations depending on the power of the heater that can be in three states: stable, neutral and unstable. Then, with solving Crank- Nicolson in different discretization coefficient, the difference was clearly seen. The effect of mesh size, Δj, has been considered and studied for three types of equations mentioned previously. It was obtained that the coarse nodalization was unable to predict the actually instability and the fine nodalization allowed predicting an unstable behavior (physical instability). Also the results showed that the explicit type is less sensitive than the other schemes. It had the weak oscillations approximately compared with others. Changing in time-step on the prediction of stability behavior has been investigated too. It was found that the oscillations were weak by decreasing Δt from 0.1 s to 0.05 s, while the effect of increasing the time-step from 0.1 s to 0.5 s is considerable. The numerical analysis of the rectangular experimental loop showed that the explicit, implicit and Crank-Nicolson schemes when applied in single-phase flow have some differences with respect to each other that are mentioned at the following:

• The range of oscillations in the results of explicit are low; in the other words a weak increase in damping can be observed by changing the mesh size compared with another scheme.

• The effect of increasing the time-step is more considerable in explicit type than implicit and Crank-Nicolson.

• The behavior of each of the three schemes appears sensitive to the changes in mesh size more than changes in time-step.

The above numerical analysis, comparing three types of finite difference solution, applied in one-dimensional single-phase flow; a further study is needed for assessing the application of the

similar schemes in two-phase flow problems. The results were obtained by CFX software too and the flow rate obtaining of numerical and CFX solutions was compared to each other. What is significant is flow reversal shown in results. The CFX software solution was compared with experimental data too. Good agreement was obtained; CFX results were more similar to experimental data than numerical.

Finally, the results of liner analysis with employing the Nyquist stability criterion showed as stability map for rectangular closed loop.

Acknowledgments

The authors are gratefully indebted to Shahid Beheshti University for partial support of this work.

References

Ambrosini, W. and Ferreri, J.C. (2000), "Stability analysis of single-phase thermosyphon loops by finite-difference numerical methods", *Nucl. Eng. Des.*, **201**(1), 11-23.

Ambrosini, W. and Ferreri, J.C. (2003), "Prediction of stability of one-dimensional natural circulation with a low diffusion numerical scheme", *Ann. Nucl. Energy*, **30**(15), 1505-1537.

Ansys, CFX. (2010), *ANSYS CFX User Manual, Computational Fluid Dynamics, Released Docs*., ANSYS Inc.

Bahonar, M. and Aghaie, M. (2017), "Study of fission gas products effect on thermal hydraulics of the WWER1000 with enhanced subchannel method", *Adv. Energy Res*., **5**(2), 91-105.

D'Auria, F. and Frogheri, M. (2002), "Use of a natural circulation map for assessing PWR performance", *Nucl. Eng. Des*., **215**(1), 111-126.

Deokattey, S., Bhanumurthy, K., Vijayan, P.K. and Dulera, I.V. (2013), "Hydrogen production using high temperature reactors: An overview", *Adv. Energy Res*., **1**(1), 13-33.

Fichera, A. and Pagano, A. (2003), "Modelling and control of rectangular natural circulation loops", *J. Heat Mass Transfer*., **46**(13), 2425-2444.

Guk, E. and Kalkan, N. (2015), "The importance of nuclear energy for the expansion of world", *Adv. Energy Res*., **3**(2), 71-80.

Huang, B.J. and Zelaya, R. (1988), "Heat transfer behavior of a rectangular thermosyphon loop", *J. Heat Transfer*, **110**(2), 487-493.

Ibrahim, Y.V., Adeleye, M.O., Njinga, R.L., Odoi, H.C. and Jonah, S.A. (2015), "Prompt neutron lifetime calculations for the NIRR-1 reactor", *Adv. Energy Res*., **3**(2), 125-131.

Jafari, J., D'Auria, F., Kazeminejad, H. and Davilu, H. (2003), "Reliability evaluation of a natural circulation system", *Nucl. Eng. Des*., **224**(1), 79-104.

Japikse, D. (1973), *Advances in Thermosyphon Technology*, in *Advances in Heat Transfer*, Elsevier, 1-11.

Kumar, M., Borghain, A., Maheshwari, N.K. and Vijayan, P.K. (2011), "Simulation of natural circulation in a rectangular loop using CFD code PHOENICS", *Kerntechnik*., **76**(2), 93-97.

Misale, M., Garibaldi, P., Passos, J.C. and De Bitencourt, G.G. (2007), "Experiments in a single-phase natural circulation mini-loop", *Exp. Therm. Fluid Sci*., **31**(8), 1111-1120.

Mousavian, S.K., Misale, M., D'Auria, F. and Salehi, M.A., (2004), "Transient and stability analysis in single-phase natural circulation", *Ann. Nucl. Energy*, **31**(10), 1177-1198.

Muscato, G. and Xibilia, M. (2003), "Modeling and control of a natural circulation loop", *J. Proc. Control*, **13**(3), 239-251.

Nayak, A.K., Vijayan, P.K., Saha, D. and Raj, V.V. (1995), "Mathematical modelling of the stability

characteristics of a natural circulation loop", *Math. Comput. Model.*, **22**(9), 77-87.
Pilkhwal, D., Ambrosini, W., Forgione, N., Vijayan, P.K., Saha, D. and Ferreri, J.C. (2007), "Analysis of the unstable behaviour of a single-phase natural circulation loop with one-dimensional and computational fluid-dynamic models", *Ann. Nucl. Energy*, **34**(5), 339-355.
Ruppersberg, J.C. and Dobson, R.T. (2007), "Flow and heat transfer in a closed loop thermosyphon Part II-experimental simulation", *J. Energy South Afr.*, **18**(4), 41-48.
Safavi, A., Abdi, M.R., Aghaie, M., Esteki, M.H., Zolfaghair, A., Pilevar, A.F. and Daryabak, A. (2012), "Study of perforated plate effect in horizontal WWER1000 steam generator", *Nucl. Eng. Des.*, **256**, 249-255.
Tolman, E.L., Kuan, P. and Broughton, J.M. (1988), "TMI-2 accident scenario update", *Nucl. Eng. Des.*, **108**(1-2), 45-54.
Tyurina, E.A. and Mednikov, A.S. (2015), "Energy efficiency analyses of combined-cycle plant", *Adv. Energy Res.*, **3**(4), 195-203.
Vijayan, P.K. (2002), "Experimental observations on the general trends of the steady state and stability behavior of single-phase natural circulation loops", *Nucl. Eng. Des.*, **215**(1), 139-152.
Vijayan, P.K. and Nayak, A.K. (2005), *Natural Circulation Systems: Advantages and Challenges*, in *Natural Circulation in Water Cooled Power Plants*.
Vijayan, P.K., Nayak, A.K., Pilkhwal, D.S., Saha, D. and Raj, V.V. (1992), "Effect of loop diameter on the stability of single-phase natural circulation in rectangular loops", *Proceedings of the 5th International Topical Meeting on Reactor Thermal Hydraulics, NURETH-5,* Salt Lake City, Utah, U.S.A., September.
Vijayan, P.K., Sharma, M. and Saha, D., (2007), "Steady state and stability characteristics of single-phase natural circulation in a rectangular loop with different heater and cooler orientations", *Exp. Therm. Fluid Sci.*, **31**(8), 925-945.
Wang, J.Y., Chuang, T.J. and Ferng, Y.M. (2013), "CFD investigating flow and heat transfer characteristics in a natural circulation loop", *Ann. Nucl. Energy.*, **58**, 65-71.
Welander, P. (1967), "On the oscillatory instability of a differentially heated fluid loop", *J. Fluid Mech.*, **29**(1), 17-30.
Zvirin, Y. (1982), "A review of natural circulation loops in pressurized water reactors and other systems", *Nucl. Eng. Des.*, **67**(2), 203-225.
Zvirin, Y. and Greif, R. (1979), "Transient behavior of natural circulation loops: two vertical branches with point heat source and sink", *J. Heat Mass Transfer*, **22**(4), 499- 503.
Zvirin, Y., Jeuck, P.R., Sullivan, C.W. and Duffey, R.B. (1981), "Experimental and analytical investigation of a natural circulation system with parallel loops", *J. Heat Mass Transfer*, **103**(4), 645-652.

CC

Nomenclature

A	Cross-sectional area(m^2)
C	Specific heat capacity
D	Diameter
f	Friction factor
g	Gravitational acceleration

Gr	Grashof number
H	Height of loop
k	thermal conductivity
L	Length
p	Constant parameter in friction factor
Q	Heat source(power)
Re	Reynolds number
q	Heat flux(W/m^2)
Pr	Prandtl number
j	Space coordinate
J	Dimensionless space coordinate
St	Stanton number
t	Time
T	Temperature
U	Secondary side conductance ($W/(m^2K)$)
V	Volume
W	Mass flow rate
z	Vertical direction coordinate

Greek letters

ρ	Fluid density
β	Thermal expansion coefficient
μ	Fluid viscosity
θ	Dimensionless temperature
ω	Dimensionless mass flow rate

Subscripts

cl	Cold leg
c	Cooler
h	Heater
hl	Hot leg
i	Node along the length of loop
n	Time step
p	Pressure
ss	Steady state
s	Secondary
t	Total
o	Reference
b	Constant parameter in friction factor
m	Modified